A simple colorimetric system for detecting target antigens by a 3-stage signal transformation-amplification strategy

*Albert M. Liao, Weihua Pan, James C. Benson, Andrew D. Wong, and G. Thomas Caltagirone**

Aptagen LLC, 250 N Main St, Jacobus, PA 17407, USA.

Keywords: Aptamer; Allosteric Ribozyme; Riboswitch; Colorimetric Detection; Isothermal Amplification; G-Quadruplex

ABSTRACT

Inexpensive, straightforward, and rapid medical diagnostics are becoming increasingly important for disease identification in time and resource-limited settings. Previous attempts at linking oligonucleotide-based aptamers and hammerhead ribozymes to form allosteric ribozymes (or riboswitches) have been successful in identifying a variety of small molecule and protein targets. Isothermal amplification reactions like EXPAR exponentially amplify minute amounts of nucleic acid templates without requiring special instrumentation. We introduce a colorimetric assay that we engineered using an aptamer, hammerhead ribozyme, EXPAR, and peroxidase activity in conjunction with a 3,3',5,5'-tetramethylbenzidine (TMB) substrate. This is a modular signal enhancer system which can be easily modified to detect virtually any chosen analyte target within 5 to 10 minutes with minimal technical requirements. Ligand-aptamer binding causes the ribozyme to change conformation and self-cleave. The cleaved riboswitch triggers exponential amplification of a reporter sequence during EXPAR. The amplification products fold into ssDNA guanine quadruplexes which exhibit peroxidase-like activity and are able to oxidize a colorless TMB substrate into a colored reaction product for visual detection. As a proof of concept, we examined the bronchodilator theophylline vs. its chemical analog, caffeine. We demonstrate linear changes in absorption readout across a wide range of target concentrations (0.5 – 1000 μM) and the ability to visually detect theophylline at 0.5 μM with approximately 35-fold increased specificity over caffeine. This 3-stage detection system is a versatile platform that will improve the rapid identification of target analytes.

Enzyme-linked immunosorbant assays (ELISAs) have been a standard laboratory technique for decades [1]. Despite their usefulness for detecting minute amounts of molecular targets or antigens, there are several limitations. ELISAs are labor-intensive and time-consuming, requiring capture of the target analyte, long incubation periods, multiple wash steps, and ultimately detection via photometric visualization [2]. These lengthy procedures coupled with reliance on sensitive laboratory equipment preclude fast detection and point-of-care testing. Rapid and sensitive detection of molecular target antigens at low concentrations can be achieved by combining the following: (1) highly selective molecular targeting, (2) signal transduction and amplification, and (3) a visually detectable readout system. Here, we introduce a novel 3-stage molecular detection system (i.e. Apta-Beacon™) using aptameric recognition and allosteric ribozymes to trigger EXPAR amplification and colorimetric output through a TMB-peroxidase substrate assay to reveal low concentrations of target analytes to the unaided eye.

Aptamers are oligonucleotide sequences, ssDNA or RNA, that can recognize and bind to molecular targets (e.g. small molecules, protein biomarkers, cells, viruses, etc.) with high affinity and specificity [3, 4]. Aptamers exhibit several exceptional advantages over antibodies, such as a longer shelf-life due to greater stability as well as easier, faster, and less expensive manufacturing/synthesis [4]. Problematic targets for antibodies, such as toxins that are poorly tolerated by animals or molecules that do not elicit a strong immune response, typically do not pose an issue for aptamer development [4]. Aptamers that specifically bind to a target can be selected from ~10^{14} – 10^{15} random oligonucleotides using a relatively simple and rapid process known as the systematic evolution of ligands by exponential enrichment (SELEX) [3]. While aptamer binding affinities are similar to those of traditional antibodies, aptamers can exhibit unparalleled target specificity. For example, Conrad et al. presented aptamers which could

distinguish between protein kinase C (PKC) isozymes that exhibited 96% homology [5]. An even more impressive display of specificity was demonstrated by the development of an aptamer that could recognize and bind to theophylline with 10,000-fold greater affinity than caffeine [6], despite their being structurally identical except for a single additional methyl group on caffeine. Although there is great potential for aptamer use in a variety of applications, including biosensors and medical diagnostics, aptamers do not directly generate an amplifiable response for rapid detection. Below, we describe our implementation of allosteric riboswitches, which can utilize aptameric recognition to trigger signal transduction.

Allosteric riboswitches can be generated by linking an aptamer to a hammerhead ribozyme structural motif [7-12]. Signal transduction is achieved by the formation of a self-cleaving ribozyme that responds to the presence of effector targets or analytes [7-12]. Allosteric riboswitches have been developed against a variety of targets such as proteins [13], biomarkers [14], and small molecules [15, 16]. Naturally occurring riboswitch classes exist as highly conserved sequences and structures with specific ligand pockets that target metabolites (e.g. amino acids, nucleobases, coenzymes, metal ions) to regulate gene expression [17]. Recent bioinformatic approaches have identified many unique riboswitch variants and highlight the potential for further discovery of molecular recognition pathways and applications [18]. Here, we use an allosteric riboswitch to trigger signal amplification—specifically an isothermal amplification reaction—following aptamer binding. Isothermal amplification exponentially replicates nucleic acid material from small starting amounts in a manner similar to PCR [19-22]. Unlike PCR, isothermal amplification does not require special instrumentation or thermocycling, and thus can be performed at constant temperature. Several reaction variants are able to linearly amplify nucleic acid targets [23]; however, exponential amplification reactions (EXPAR) utilize their

oligonucleotide products to prime new reaction templates and thus perform rapid exponential amplification [21]. Therefore, to achieve signal transduction and rapid molecular amplification, we use allosteric riboswitches to translate an aptamer binding event into a trigger for an EXPAR-compatible nucleic acid response.

While EXPAR can be used to amplify virtually any oligonucleotide sequence exponentially, specific oligo templates were used to generate guanine quadruplexes (GQ) that can form a peroxidase-mimicking DNAzyme with hemin [24]. Upon the addition of hemin and peroxide, GQ forms an active DNAzyme that is capable of oxidizing tetramethylbenzidine (TMB) to produce a visible color change. Here, we introduce a sensitive colorimetric detection system (i.e. Apta-Beacon™) to identify the presence of an analyte through EXPAR and TMB oxidation triggered by target-specific allosteric riboswitch activity.

As a proof of concept and to demonstrate both specificity and sensitivity, we developed an Apta-Beacon™ for the small molecule theophylline. Theophylline is a bronchodilator commonly used for the treatment of asthma and chronic obstructive pulmonary disease (COPD) and produces a therapeutic effect at plasma levels between 20 - 100 μM; however, dosing must be closely monitored since the risk of adverse drug reactions occurs above this narrow therapeutic range, and theophylline clearance and pharmacokinetics varies from patient-to-patient [25]. Clinical analysis of theophylline concentrations in plasma or serum relies on high performance liquid chromatography (HPLC) or commercial immunoassays [26, 27], which are time-consuming and prone to overestimating levels due to interference from structurally similar caffeine and theobromine [26, 28]. Our assay uses a previously developed riboswitch capable of discerning between theophylline and caffeine [8]. Upon recognition of theophylline, the riboswitch self-cleaves and triggers EXPAR amplification of GQ DNAzymes that oxidize TMB

and enable the colorimetric detection and visual discernment of theophylline from caffeine at concentrations as low as 0.5 μM. In addition to rapid visual detection, this platform also enables precise quantification of theophylline concentrations through time-dependent linear changes in absorption. By customizing the aptamer recognition unit bound to the riboswitch, this visual detection system can be applied to virtually any target analyte of interest, thus providing a modular platform for the rapid detection and quantification of molecular targets for which traditional ELISA assays may not provide sufficient sensitivity or speed.

Material and Methods

Oligonucleotides. Sequences of riboswitch constructs are presented in Table S1. Single-stranded DNA molecular weight marker (20/100 ladder) was purchased from Integrated DNA Technologies, Inc (Coralville, IA 52241, USA). All DNA nucleotide sequences (Tables S2, S3, and S4) were synthesized and desalted by Integrated DNA Technologies, Inc (Coralville, IA 52241, USA). Full-length oligonucleotides were assembled using Titanium® Taq (2 μM primers, 200 μM dNTPs, initial denaturation for 3 minutes at 94 °C, cycles of 30 seconds at 94 °C, 40 seconds at 52 °C, 60 seconds at 72 °C, final extension of 5 minutes at 72 °C). RNA was transcribed using Ampliscribe™ T7 Transcription Kits according to kit protocols, and purified using 10% denaturing PAGE with 8 M urea. Secondary structures for riboswitches were depicted using VARNA interactive drawing software [29].

Kits and enzymes. Titanium® Taq PCR Kit was purchased from Clontech Laboratories, Inc. (Mountain View, CA 94043, USA). AmpliScribe™ T7 Transcription Kit was purchased from Epicentre Biotechnologies (Madison, WI 53719, USA). Nicking endonucleases (Nt.BstNBI),

DNA polymerases (Bst. 2.0), and T4 polynuceotide kinase were purchased from New England Biolabs, Inc. (Ipswich, MA 01938, USA).

Reagents. Theophylline (THE), caffeine (CAF), flavin mononucleotide (FMN), hemin, hydrogen peroxide solution (H_2O_2, 30 wt. % in H_2O) and TMB (3,3',5,5'-tetramethylbenzidine dihydrochloride) were purchased from Sigma-Aldrich Corp. (St. Louis, MO 63103, USA). Hemin stock solution (5 mM) was prepared in DMSO (AMRESCO LLC, Solon, OH 44139, USA), stored at -20 °C in the dark, and used within one month. TMB stock solution was prepared by dissolving 1 tablet TMB (1 mg) in 8.33 ml 100 mM sodium phosphate pH 6.0 (NaH_2PO_4) and stored at 4 °C in the dark. All other reagents were prepared with Molecular Biology-Grade USP Sterile purified water from Corning, Inc. (Corning, NY 14831, USA) and stored at -20 °C.

Apparatus. Riboswitch template construction and quantitation were performed using a PTC-100 programmable thermal cycler (MJ Research Inc., Bruno, J3V4P1, Canada), PAGE equipment (C. B. S. Scientific Co., Del Mar, CA 92014, USA), and ND-1000 UV/Vis spectrophotometer (NanoDrop Technologies, Inc., Wilmington, DE 19810, USA).

Riboswitch reactions. Riboswitch reactions in Stage 1 for all constructs were conducted using 240 nM riboswitch (i.e. RS-TFU76, RS-TFU107, RS-FMN72, etc.) with target (i.e. THE, CAF, or FMN) concentrations ranging from 0.100 – 1500 μM, unless otherwise indicated. T4 nucleotide kinase mix is comprised of 0.5 μL of water and T4 polynucleotide kinase (10 U/μL) with 1 μL of 10X T4 nucleotide kinase buffer (700 mM Tris-HCl at pH 7.6, 100 mM $MgCl_2$, 50 mM DTT). Reactions were initiated by combining 1 μL T4 nucleotide kinase mix, 1 μL 5X reaction buffer (250 mM Tris-HCl at pH 7.5 and 100 mM $MgCl_2$), and 2 μL of 600 – 2400 nM riboswitch (in nuclease-free water) in the presence or absence of 1 μL target. After an indicated

length of time, reactions were terminated by chilling on ice. Following reactions, 2.5 μL was used for denaturing PAGE analysis.

G-quadruplex-exponential amplification reaction (GQ-EXPAR). 12 pmoles of each ssDNA template (p3tq49 and qtq47) were added to 35 μL reaction buffer, which contained 40 nmoles dNTPs (8 nmoles dATP, 4 nmoles dCTP, 24 nmoles dGTP, and 4 nmoles dTTP, optimized for G-rich EXPAR products), 64 units Nt.BstNBI nicking endonuclease, 1.6 units Bst 2.0 DNA polymerase, 2 μL 10X Isothermal Amplification Buffer (200 mM Tris-HCl, 100 mM $(NH_4)_2SO_4$, 500 mM KCl, 20 mM $MgSO_4$, 1% Tween® 20, pH 8.8 at 25 °C) and 2 μL 10X NEBuffer 3.1 (1 M NaCl, 500 mM Tris-HCl, 100 mM $MgCl_2$, 1 mg/mL BSA, pH 7.9 at 25 °C) (Soukup et al., 2000). GQ-EXPAR was initiated by combining 2.5 μL of riboswitch-reaction to 17.5 μL of this pre-mixture in thin-wall PCR tube strips. These samples were incubated at 55 °C for indicated times with a preheated metal block (85 °C) laid on top of the tube strips to prevent evaporation. Reaction was terminated by chilling on ice. Reaction product (2.5 μl) was used for 10% denaturing PAGE (8 M Urea) analysis.

Tetramethylbenzidine (TMB) redox. GQ-EXPAR reaction product (2.5 μL) was combined with 2.5 μL of Hemin-KCl solution (4 μM Hemin, 25 mM KCl; prepared fresh for each trial) and 95 μL TMB-H_2O_2 solution (0.12 mg/mL TMB, 18 mM H_2O_2, 100 mM NaH_2PO_4-Na_2HPO_4 at pH 6.0) to initiate the GQ-Hemin (DNAzyme) catalyzed TMB redox reaction. Reactions were carried out at 23 °C for indicated times. Photographs were taken in a light box under ambient light using a Samsung WB350F digital camera.

Lower Limit of Detection Analysis. In Stage 1, 240 nM of riboswitch (RS-TFU107) was incubated with 0.48 – 1500 μM theophylline in 1X reaction buffer with a 1:10 dilution of T4 nucleotide kinase mix for 3 minutes at 23 °C. A buffer-only control (i.e. no theophylline) and a

riboswitch-only control (i.e. no theophylline, no buffer) were also assayed. Reactions were stopped by transferring to ice and combined with 70 µL of EXPAR pre-mixture. Samples were divided into three 20 µL aliquots to undergo EXPAR at 55 °C for 5 minutes. Each sample was combined with 1 µL of hemin-KCl solution and 29 µL of TMB-H_2O_2 solution, then incubated for 3 minutes at 23 °C for color development. Color development was stopped with 20 µL of 2 M H_2SO_4, and samples analyzed for absorbance at 450 nm (Flexstation 3 Microplate Reader, Molecular Devices, Sunnyvale, CA) at room temperature.

Results

Mechanism of 3-Stage Detection System. This aptamer-based bio-detection system is made up of three separate stages which have been outlined in Figure 1.

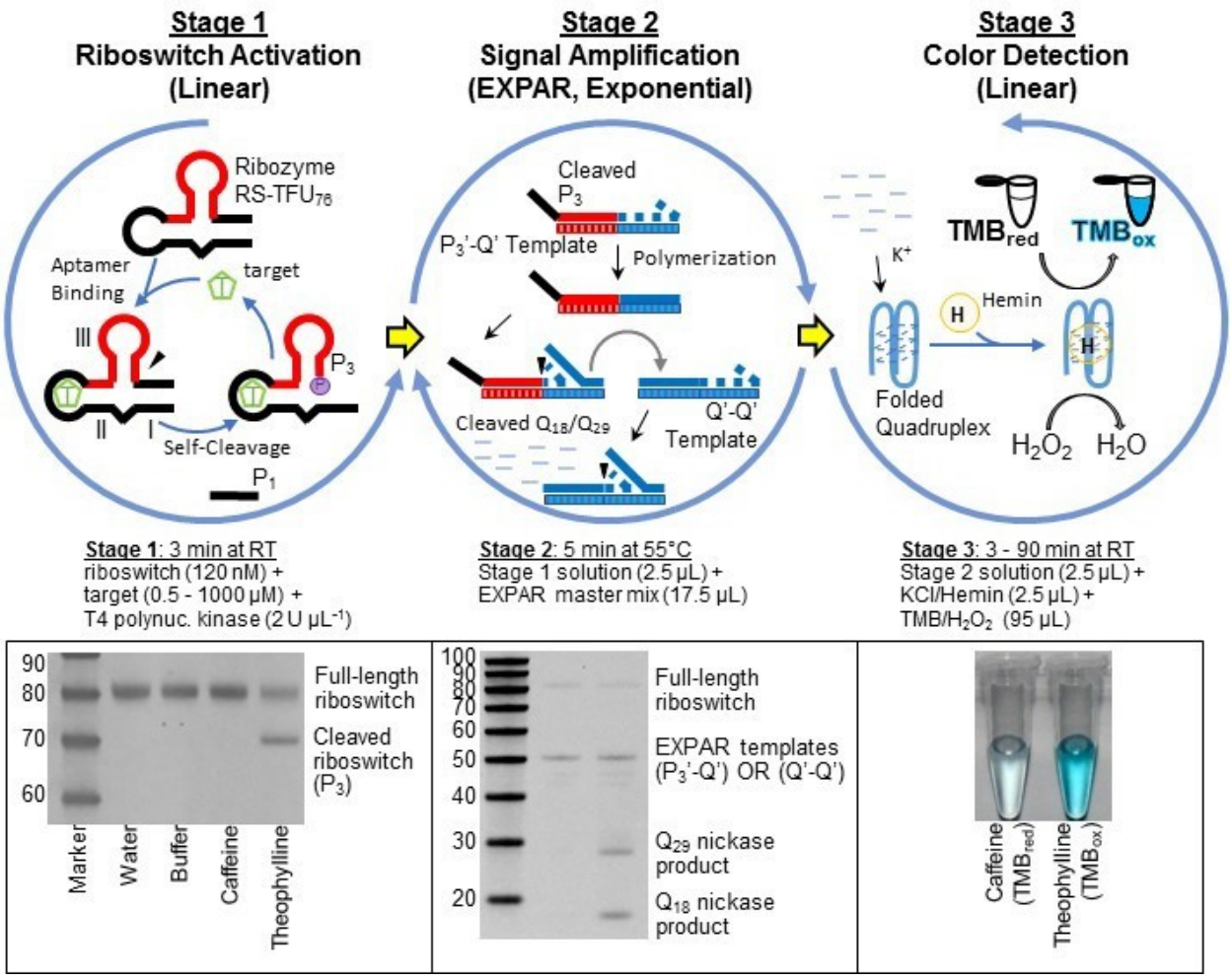

Figure 1. Allosteric riboswitch – GQ-EXPAR system overview. (Stage 1) Effector ligand/theophylline target (T) binds to aptamer domain linked to a cis-acting hammerhead ribozyme (RS-TFU76), inducing the conformational change to the "ON" state and subsequent self-cleavage that forms two products, P1 and P3. T4 polynucleotide kinase reduces the 2',3'-cyclic phosphate on P3 to a terminal 3'-hydroxyl, thus producing an active site for EXPAR initiation. Representative denaturing PAGE gel showing the resulting cleaved product (P3) in the presence of theophylline (1 mM) (bottom). (Stage 2) EXPAR amplification is initiated by the cleaved kinase-treated ribozyme (P3) and from the given templates produces ssDNA guanine quadruplex precursors (Q). Representative denaturing PAGE gel showing development of Q

(bottom). (Stage 3) ssDNA Q folds in the presence of potassium (K+) and associates with hemin (H) to generate peroxidase activity. Color is developed as the clear 3,3',5,5'-tetramethylbenzidine (TMBred) substrate is oxidized to a blue state (TMBox). Representative color development in tube strips (bottom).

The riboswitch involved in Stage 1 is comprised of an aptamer domain and a *cis*-acting hammerhead domain bridged by a communication module in stem II (RS-TFU76, Fig. 2A).

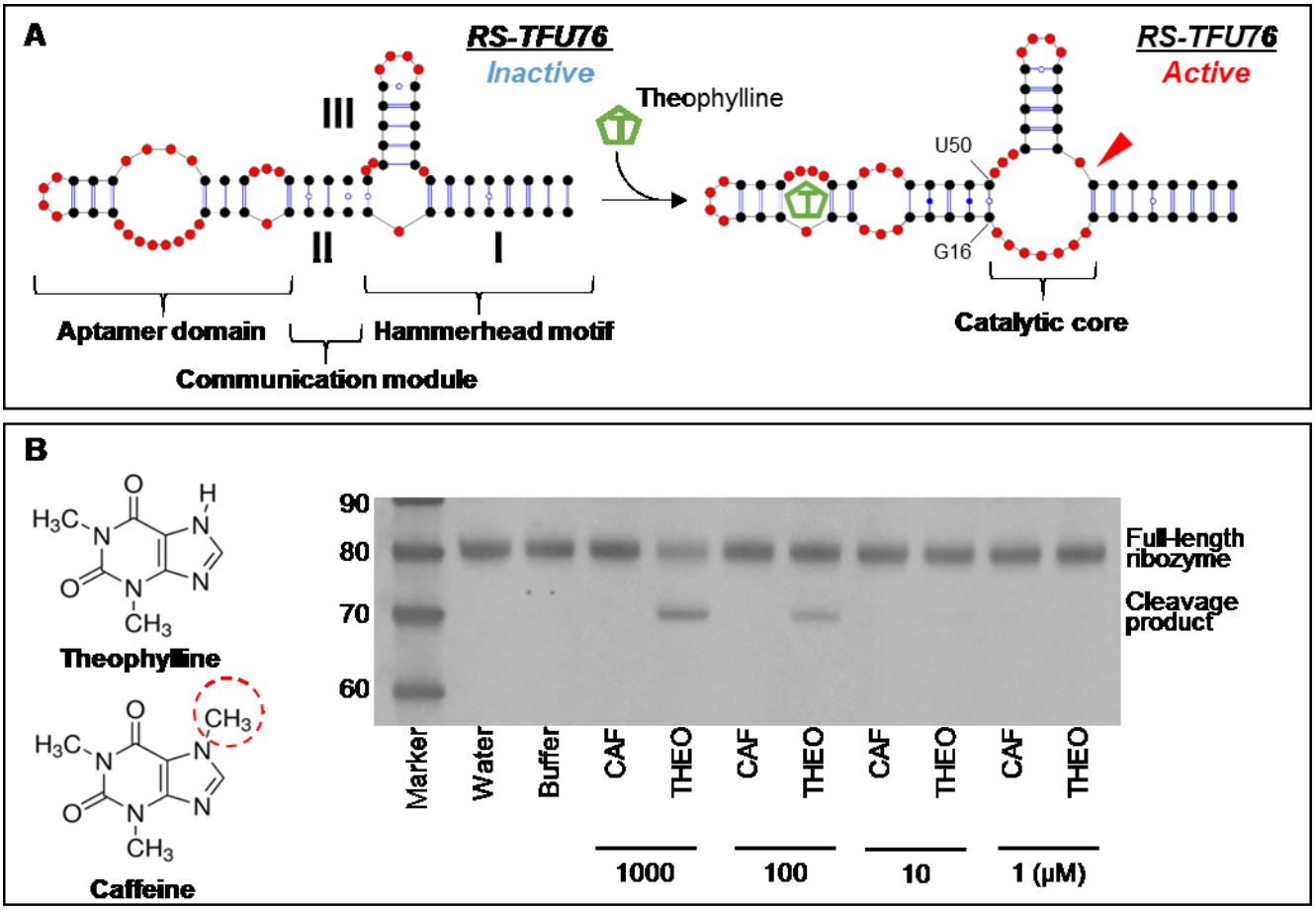

Figure 2. Allosteric riboswitch targeting, activation, and self-cleavage. (A) Inactive modified theophylline riboswitch (RS-TFU76) with aptamer-binding domain (left, stem II), communication module (middle, stem II), and hammerhead ribozyme motif (right, stems I and III). Theophylline (T) adheres to putative binding site and activates RS-TFU76 (right). Hammerhead ribozyme self-cleavage site indicated by red arrowhead. (B) (Left) Subtle molecular difference between

theophylline and caffeine indicated by red dashed circle. (Right) 10% denaturing PAGE of RS-TFU76 reactions. DEPC-treated water only and reaction buffer only reactions used as negative controls. Reactions against caffeine (CAF) and theophylline (THEO) from 1000 to 1 μM. Assays performed at 23 °C for 3 min with 0.5 μM riboswitch.

Originally adjacent to the catalytic core of the riboswitch was a G16-C50 pairing in stem II that maintains cleavage activity and defines the boundary of the catalytic core [30, 31]. This base pair has been modified during the course of our studies to G16-U50 to improve the specificity of the system (Fig. S1). The native state of the riboswitch (Fig. 2A) does not maintain the G16-U50 pairing, resulting in a largely inactive switch in the "OFF" conformational state. When theophylline populates the aptamer domain in Stage 1, the domain structurally transforms, causing a rearrangement of the stem II communication module [30, 31] and restoring the G16-U50 base pair. This causes hammerhead ribozyme activation, changing to the "ON" conformational state and leading to self-cleavage (Fig. 2A) [8]. Self-cleavage causes the riboswitch to open and create two cleavage products (i.e. P_1 and P_3) (Fig. 1). P_3, the larger of the two cleavage products, exhibits a new 3'-end containing a 2',3'-cyclic phosphate, and the addition of T4 polynucleotide kinase is able to reduce the cyclic phosphate so that P_3, acting as a "trigger", can initiate 5' to 3' polymerization in EXPAR for Stage 2 [32, 33]. Although P_1 could also be used to trigger EXPAR in Stage 2, its location at the end of Stem I (Fig. 2A) is predisposed to "breathing", or reversible base-pair dissociation, and this kinetically induced exposure of the P_1 sequence can prematurely trigger EXPAR without self-cleavage or analyte detection. As such, P_1 does not participate further in subsequent stages. Theophylline is not consumed during riboswitch activation and cleavage, therefore it can be released by the aptamer domain and become available to bind to another riboswitch in Stage 1.

During EXPAR in Stage 2 [34], Bst 2.0 polymerase extends P_3 into a quadruplex precursor segment (Q_{18}) using a P_3'-Q' template (Table S4). The nicking enzyme Nt.BstNBI cleaves the newly polymerized Q_{18} from the P_3 trigger, allowing Q_{18} to dissociate or be displaced by another unit of Bst 2.0 polymerase that re-extends the P_3 segment. This allows the regenerated primer-template to continually generate Q_{18} at a linear rate. After dissociation, the generated Q_{18} segments either prime the Q'-Q' template for exponential amplification of additional Q_{18} or self-fold into G-quadraplexes upon the addition of potassium in stage 3.

In Stage 3, the G-quadraplexes self-assemble with hemin into an active DNAzyme, which uses TMB as a proton donor to reduce H_2O_2 to H_2O. The oxidation of TMB causes a color change in the solution, progressing from clear to blue to yellow.

Aptamer sensitivity and specificity. Caffeine, which structurally differs from theophylline by only a single methyl group (Fig. 2B), was used as a control to test the specificity of the detection system [6]. The theophylline riboswitch alone has been reported to exhibit ≈400-fold greater affinity towards theophylline vs. caffeine, with a K_d of 15 μM [8]. When verifying riboswitch-only detection results by denaturing PAGE, we observed un-cleaved riboswitch as a 76 nt band and cleaved riboswitch as a 68 nt band (P_3), while the shorter cleaved off segment of the riboswitch (P_1) ran off the gel (Fig. 2B). Despite incubation at concentrations at 1 - 1000 μM, caffeine does not initiate appreciable levels of ribozyme cleavage whereas theophylline produces a concentration dependent cleavage response. At 1 mM, theophylline is able to cleave a significant fraction of the full-length ribozyme in only 3 min at room temperature.

EXPAR reaction and color development. Following 1 mM target (i.e. theophylline) and control (i.e. caffeine, buffer) reactions with 240 nM ribozyme (RS-TFU76) for 1 min, cleavage product (P_3) from Stage 1 was subjected to EXPAR for 3 - 6 min (Fig. 1). Half of the reacted

material in Stage 2 was used for PAGE analysis (Fig. 3A), and the remaining half was used for GQ color development (Fig. 3B). Full-length EXPAR products are evident as 47 nt and 49 nt bands during PAGE analysis (Fig. 3A), while the nickase-cleaved EXPAR products (i.e. Q_{18} and Q_{29}) manifest as 18 nt and 29 nt products. PAGE specificity for theophylline was determined for 3 - 6 minute EXPAR reaction times. Caffeine served as a control to assess background amplification and specificity of the reaction.

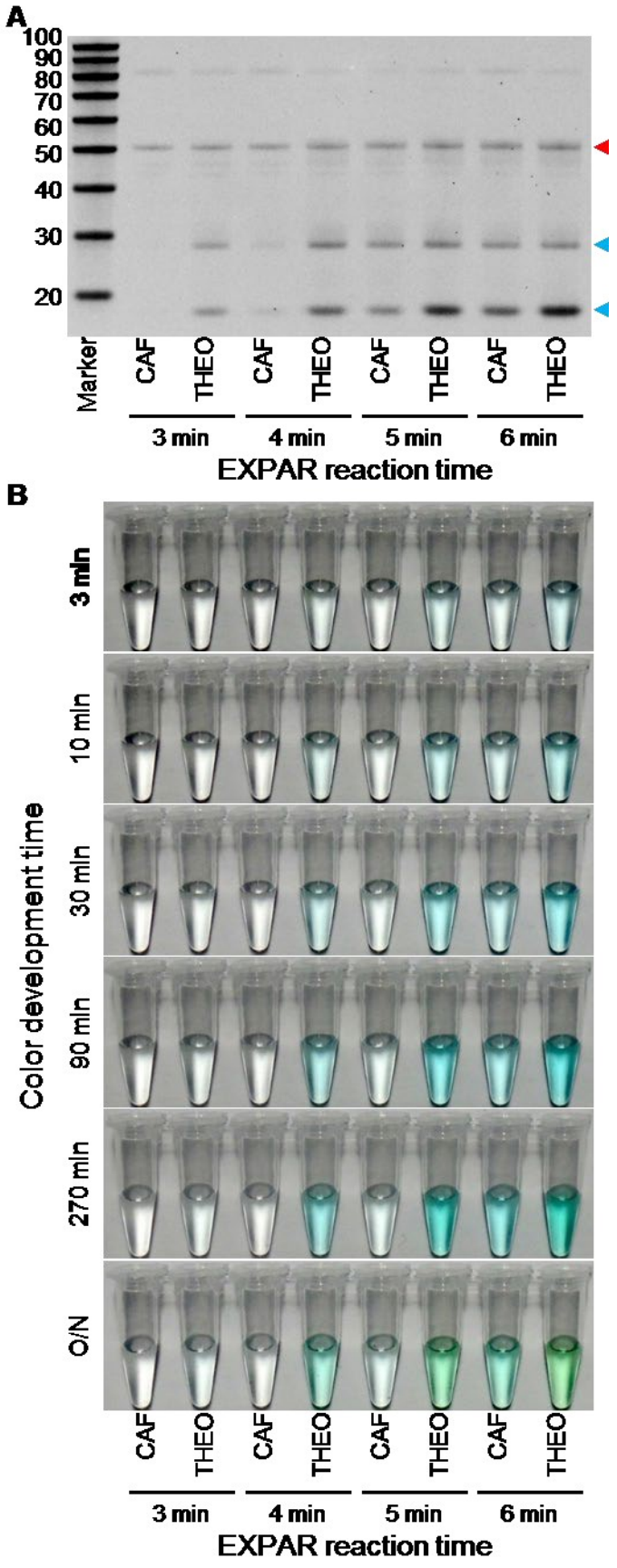
A
100
90
80
70
60
50
40
30
20
Marker
CAF
THEO
CAF
THEO
CAF
THEO
CAF
THEO
3 min
4 min
5 min
6 min
EXPAR reaction time
B
Color development time
3 min
10 min
30 min
90 min
270 min
O/N
CAF
THEO
CAF
THEO
CAF
THEO
CAF
THEO
3 min
4 min
5 min
6 min
EXPAR reaction time

Figure 3. Effect of EXPAR incubation time on GQ generation and color development. (A) EXPAR conducted for the indicated times using activated riboswitch (RS-TFU76) from Stage 1 incubation with 1 mM theophylline or caffeine. Half of each EXPAR reaction analyzed on denaturing PAGE. Red arrowhead indicates the pre-cleaved EXPAR product as well as template; blue arrowheads indicate the nicking products (Q18 and Q29) generated during isothermal amplification. (B) The remaining half of each EXPAR reaction product was used for color development of 3 min to overnight (O/N).

Caffeine exhibits "background" EXPAR reaction products with increasing reaction time (Fig. 3A). The effects of buffer alone were similar to caffeine controls at EXPAR reactions times greater than 3 min (Fig. S2A). EXPAR in the absence of initiator oligos has been shown to suffer from early phase non-specific background amplification that may not be completely explained by contamination and primer-dimer formation, but may be due to polymerase/template interactions [35]. Optimization was conducted (Figs. S3 and S4) using a previously successful method to design EXPAR templates (Table S4) that minimize background amplification [24] while considering optimal GQ length (Fig. S5A). Denaturing PAGE analysis after EXPAR shows that theophylline will generate about 1.5- to 5-fold more product in Stage 2 than equal amounts of caffeine or buffer given EXPAR reaction times of 3 - 5 minutes (Fig. 3A). At EXPAR reaction times greater than 5 minutes, non-specific background amplification limits the reliable discernment of theophylline from caffeine (Fig. 3A).

To demonstrate color development following EXPAR, GQ-EXPAR products were combined with color development solutions (see Materials and Methods) to a final concentration of 0.1 μM hemin, 0.114 mg/mL TMB, and 17.1 mM H_2O_2. Color progressed from clear to blue based on the amount of EXPAR product and development time. A 3 min EXPAR reaction time was not

sufficient to generate adequate product for color development (Fig. 3B). EXPAR reaction times greater than or equal to 4 min, in combination with color development times as short as 3 min, enabled visual discernment between theophylline and caffeine. For longer EXPAR and color development times, color progressed from blue to green (Fig. 3B) and eventually yellow (Figs. S5 and S6).

At the shortest EXPAR time tested, 3 min, visual colorimetric differences could not be noted until 90 min of elapsed color development time (Fig. 3B). Colorimetric differences between 1 mM theophylline and caffeine could be faintly detected by eye in as little as 4 min EXPAR time and 3 min color development time (Fig 3B). These results demonstrate the rapidity by which outcomes from this test can be attained, an important attribute for a medical diagnostic that informs urgent or time-sensitive treatment.

Establishing practical minimal target quantity. To increase sensitivity at lower target concentrations, we incubated RS-TFU76 with theophylline for longer periods of time, thus increasing the reaction time in Stage 1 and cleaved product (P_3) entering Stage 2. Performing a Stage 1 reaction time of 3 min (Fig. 4), instead of 1 min (Fig. 3), increased the amount of cleaved riboswitch product detected in PAGE gels (Figs. 3A and 4A) and resulted in shorter color development times (Figs. 3B and 4B) despite being incubated with a ten-fold lower concentration of theophylline or caffeine. Colorimetric differences between theophylline and caffeine could be discerned after 3.5 - 4 min EXPAR reaction times, but specificity markedly decreased at 5 min (Fig. 4B). Due to the high specificity of riboswitches, increasing the incubation period in Stage 1 is able to more efficiently improve the lower detection limit rather than extending EXPAR time in Stage 2, which is prone to non-specific background amplification.

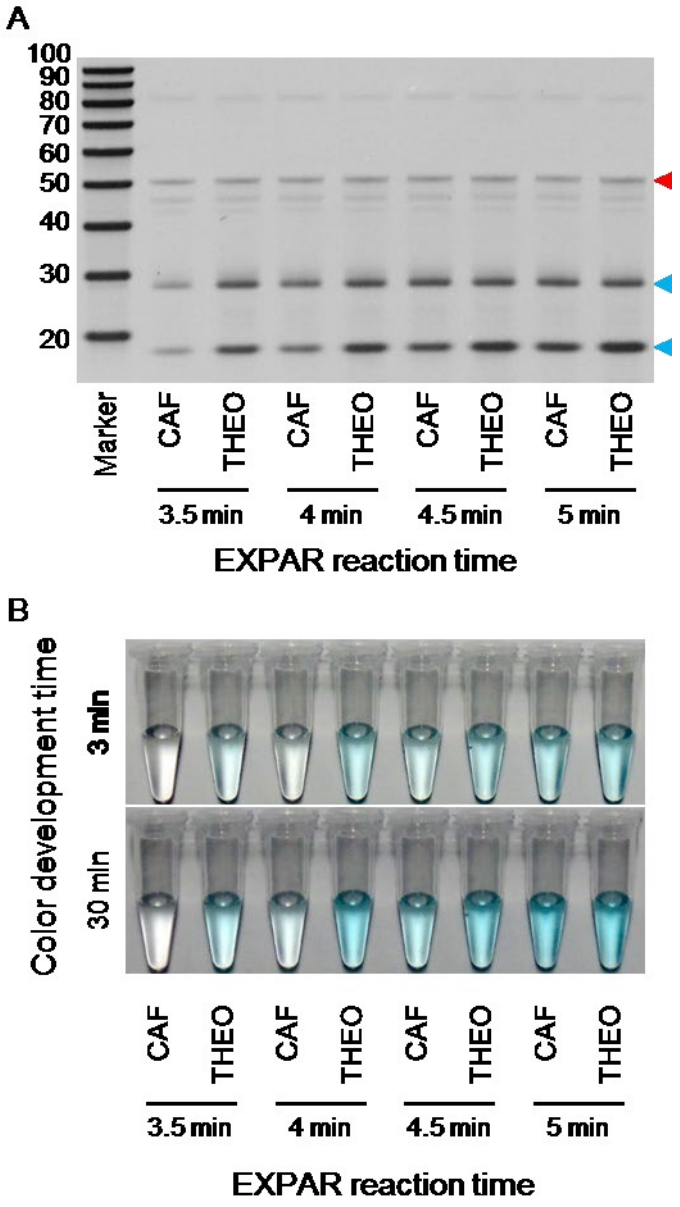

Figure 4. Higher-resolution examination of color development by GQ derived from RS-TFU76-EXPAR. (A) Reactions were performed using a final concentration of 240 nM TFU76 combined with 100 µM caffeine or theophylline, and were incubated at 23 °C for 3 min; followed by EXPAR incubations at 55 °C for 3.5 to 5 min as indicated. Half of the EXPAR reaction products were analyzed on 10% denaturing PAGE with 8 M Urea. The red arrowhead indicates the pre-cleaved EXAPR product and template, and the blue arrowheads indicate the nicking products generated

during isothermal amplification. (B) The remaining half of the EXPAR reaction products were used for color development over the indicated times.

To further improve the lower detection limit, we increased the sensitivity for theophylline in Stage 1 by utilizing RS-TFU107 (Table S1). This construct differs from RS-TFU76 by containing a total of 22 bp on its stem I (SI) with a three-base overhang. RS-TFU76 exhibits only 8 bp on SI, which likely produces a lower stability structure with higher background due to steric interactions between stem I and II [11, 36]. RS-TFU107 exhibited stronger detection of 10 μM theophylline than RS-TFU76 (Figure S7), and the additional stability provided by the 22 bp SI enabled 0.5 μM theophylline detection (Fig. 5). At 10 μM target concentration, we could rapidly distinguish between theophylline and caffeine (i.e. 3 min riboswitch reaction, 4 min EXPAR, and 3 min color development) (Fig. 5A). Lower analyte concentrations could be visually detected by simply increasing the color development time while keeping the same conditions in Stages 1 and 2. For example, to visualize colorimetric differences between theophylline and caffeine at the lowest tested target concentration, 0.5 μM, color development time was increased to 30 min (Fig. 5A). While visual discernment of lower target concentrations may be achieved with longer color development times, the current system is amenable to faster and more quantitative detection by utilizing an absorbance plate reader to measure differences in H_2SO_4-stopped samples (to stop the color development reaction and maintain equal color development time between samples) that are unperceivable to the naked eye (Fig. 5B). Thus, in addition to demonstrating the visual detection of clinically relevant levels of theophylline (20 - 100 μM), this 3-stage system also enables the fast and precise quantification of a wide range of theophylline concentrations (0.5 - 1000 μM) by measuring absorbance (Fig. 5B).

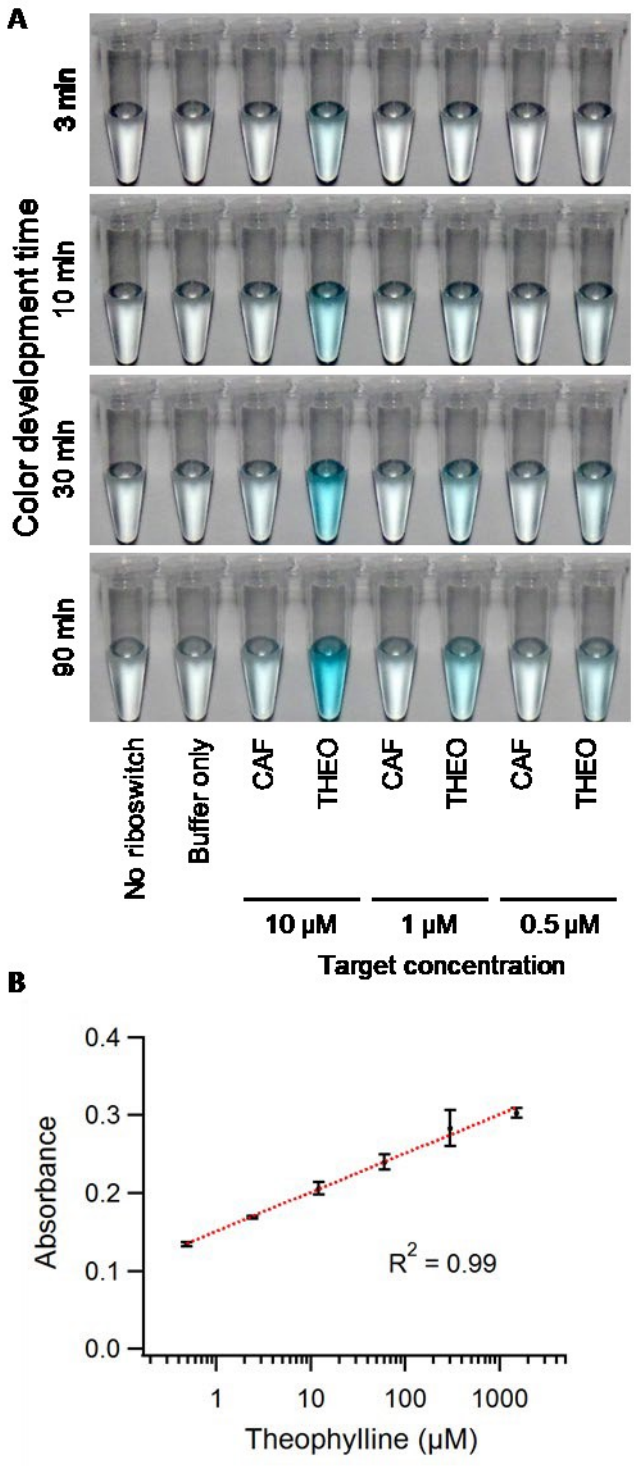

Figure 5. Lower limit of detection for RS-TFU107. (A) Colorimetric output from 3-stage detection system against varying target concentrations with a Stage 1 incubation time of 3 min. System produces visually discernible differences in color development against as little as 0.5 µM

theophylline (THEO) over caffeine (CAF) within 30 minutes of color development. Reactions were performed using a final concentration of 240 nM TFU107 combined with 0.5 -10 μM of either CAF or THEO, and were incubated at 23 °C for 3 min. EXPAR incubations were conducted at 55 °C for 4 min, and the color was allowed to develop for up to 90 min, as indicated at left of the tube strips. (B) Linear absorbance readout of THEO target concentrations on semi-log plot of H2SO4-stopped color development. Results at each concentration represent mean ± SE (n = 3).

Discussion

Molecular amplification for enhanced sensitivity. Aptamers have been developed through the SELEX process to complement and/or replace antibodies in ELISA detection systems [37]. While these molecular detection schemes have demonstrated the benefits of incorporating systematically engineered aptamers, they are limited by their dependence on photometric detection and long assay durations [2]. Colorimetric systems have been developed that utilize aptamer recognition to trigger a visible color change through the induced aggregation of metal nanoparticles and changes in surface plasmon resonance [38, 39]. In principle, these systems provide visual detection and rapid processing times; in practice, they lack signal amplification to enable the visual discernment of lower concentration limits of targeted analytes, and ultimately require photometric detection for concentrations below 250 μM of theophylline [40]. Aptamer binding and signal transduction for triggered molecular amplification and detection has recently been demonstrated for the biosensing of PGDF-BB and adenosine at lower limits of 0.38 fM and 48 nM respectively; however, the implementation of strand displacement amplification and N-methyl mesoporphyrn IX limits the rapidity of the assay to hours and quantitation relies on fluorescence detection [41]. Substituting a fluorescent substrate in Stage 3, rather than triggering a

colorimetric output, can further improve the lower detection limit of the herein described system, but increases the equipment burden for detection. Here, we incorporate signal transduction and rapid amplification in Stages 1 and 2 that can be tuned to increase the visible readout in Stage 3 within minutes for clinically relevant concentrations of theophylline (20 - 100 μM). We have demonstrated that longer incubation times between a high specificity, self-cleaving riboswitch and target analyte in Stage 1 resulted in more cleaved product to initiate EXPAR in Stage 2, and thus improved signal amplification to visually detect lower limits (0.5 μM) in Stage 3 (Fig. 5). The incorporation of a well-defined amplification stage is key for generating a robust molecular response that provides a visual readout in real-time.

Practical application for medical diagnostics and theragnostics. Theragnostics is the ongoing diagnostic monitoring of patients during treatment of a disease or condition and subsequent modulation of drug dosage based on response [42]. Fast and accurate theophylline monitoring during treatment may reduce the risk of overdose and improve the clinical management of COPD and asthma [28, 43]. Typical sandwich ELISA procedures result in an assay duration of approximately 6 – 20 hours [37]. Here, we have demonstrated the visual detection of pharmacologically relevant levels of theophylline within minutes (Fig. 5). Rapid and inexpensive technologies have enabled the emergence of low cost, point-of-care diagnostic devices [2]. The most familiar diagnostic platforms include electrochemical and lateral flow assays [44] and paper strips [45]. Several commercialized diagnostics utilize microfluidics to miniaturize these platforms and reduce reagent cost; however, they often require portable analyzers or workstations to automate sample processing and detection to realize the technology in a point-of-care setting [46, 47]. Our assay requires relatively minimal expertise and fluid handling steps to mix preloaded volumes between Stages 1 – 3 and a heating element to maintain

a 55 °C reaction temperature for ≈5 min during Stage 2 (Fig. 1). While this 3-stage detection system can be readily adapted for automation and precise quantitation (Fig. 5B), we have demonstrated the fast and sensitive detection of theophylline by eye without sophisticated back-end equipment or benchtop systems. Although exogenous RNA and riboswitches are highly susceptible to degradation in plasma [48], the addition of RNase inhibitor has been shown protect RNA aptamer functionality for the electrochemical detection of theophylline [26].

Previously, a molecular sensor system was engineered using an allosteric riboswitch coupled with a fluorophore, quencher dye, and double-labeled RNA substrate, in which riboswitch activation by aptamer-ligand binding was coupled with fluorescence quencher removal and thus fluorescence increase [7]. Sensitivity was demonstrated for theophylline concentrations ranging from 0.01 to 2 mM [7]. However, unlike the colorimetric system described in this work, in which differences between samples can be easily discerned visually, the fluorescence-based system required a UV light source for result detection. While certain diagnostics offer concurrent multiplex detection against several different analytes [49], they require sensitive photometric equipment for readout. As such, the herein developed colorimetric system is more practical for limited laboratory and point-of-care settings.

Adaptability of 3-Stage Detection System. Since the aptamer recognition unit of the riboswitch can be interchanged, this system can be adapted to detect virtually any targets capable of aptamer detection while riboswitch functionality is maintained. As an additional proof of concept, we have adapted a pre-existing riboswitch for the detection and colorimetric output of flavin mononucleotide (FMN) (Fig. S1 and S2). Our system has practical applications in many medical diagnostic tests, especially those requiring high sensitivity and/or rapid processing times to inform critical medical treatments, such as immune-mediated type II heparin-induced

thrombocytopenia (HIT-II) [50], pertussis [51], troponin [52], syphilis [53], Ebola [54], and Lyme disease [55] among others. Aptamers have been developed for the detection of HIT-II [56], troponin [57], syphilis [58], and Ebola [59], and can be readily implemented in our colorimetric amplification system for medical diagnostic usage. Additionally, the ease with which aptamers can be screened and produced for nearly any analyte and utilized in this format may result in the widespread development of easy, rapid diagnostic tools for a multitude of infectious disease and theragnostic applications. The 0.5 μM detection limit for this system serves as a strong basis for further optimization to reduce assay duration, determine detection limits with samples from human serum, and achieve a level of sensitivity comparable to that of existing immunoassays (fM – nM) [47]. Substituting a fluorescent substrate, such as QuantaBlu™ or QuantaRed™ (Thermo Fisher Scientific; Waltham, MA), AmplifluRed™ (Sigma-Aldrich; St. Louis, MO), or H_2DCFDA, in Stage 3 should improve the lower limit of detection and further demonstrates the advantages of the herein described 3-stage detection system that enables relatively simple customization by interchanging individual stages.

Conclusions

We engineered a medical diagnostic assay consisting of an aptamer, hammerhead ribozyme, and GQ-EXPAR reaction. The target analyte binds to the aptamer, causing ribozyme cleavage that initiates an EXPAR reaction. The resulting amplified DNA sequences form GQs and bind to hemin to trigger a peroxidase-supported colorimetric reaction that develops a visible color change from clear to blue. The results from this system can be obtained in a short amount of time with limited equipment and can be visualized via a straightforward colorimetric output. We have demonstrated a visual diagnostic capable of discerning between theophylline and its

chemical analog caffeine at concentrations as low as 0.5 μM. The advantages of SELEX derived aptamers over antibodies, coupled with the ease with which our system can be re-engineered, allows for this test to be tailored for nearly any aptamer targeted analyte.

Acknowledgements

We thank Dr. Richard Bamford for his assistance in testing initial protocols of the GQ-EXPAR system. We are also grateful to Dr. Gregory Yourek for his efforts in the initial arrangement of information in preparing this manuscript.

ASSOCIATED CONTENT

Supporting Information

Supporting Information is available free of charge on the [WEBSITE]. Provided information includes the sequences of DNA and RNA riboswitches, primers, and templated, data on riboswitch catalytic activity, denaturing PAGE analysis of reaction products, and comparison of color development progression due to various parameters.

AUTHOR INFORMATION

Corresponding Author

*Corresponding author. Tel/Fax: +1 717 278 2436. E-mail address: tom@aptagen.com

Author Contributions

The manuscript was written through contributions of all authors. All authors have given approval to the final version of the manuscript.

Funding Sources

This research was supported with internal funding by Aptagen, LLC. G.T.C. is the president and CEO of Aptagen, LLC. A.M.L., W.P., and J.C.B. are employed by Aptagen. A.D.W. is a scientific advisor with Aptagen. Apta-beacon™ is a trademarked assay platform developed by Aptagen.

REFERENCES

1. Gan, S. D., and Patel, K. R. (2013) Enzyme immunoassay and enzyme-linked immunosorbent assay, *The Journal of investigative dermatology 133*, e12.
2. Respess, R. A., Rayfield, M. A., and Dondero, T. J. (2001) Laboratory testing and rapid HIV assays: applications for HIV surveillance in hard-to-reach populations, *Aids 15 Suppl 3*, S49-59.
3. Tuerk, C., and Gold, L. (1990) Systematic evolution of ligands by exponential enrichment: RNA ligands to bacteriophage T4 DNA polymerase, *Science 249*, 505-510.
4. Jayasena, S. D. (1999) Aptamers: an emerging class of molecules that rival antibodies in diagnostics, *Clin Chem 45*, 1628-1650.
5. Conrad, R., Keranen, L. M., Ellington, A. D., and Newton, A. C. (1994) Isozyme-specific inhibition of protein kinase C by RNA aptamers, *J Biol Chem 269*, 32051-32054.
6. Jenison, R. D., Gill, S. C., Pardi, A., and Polisky, B. (1994) High-resolution molecular discrimination by RNA, *Science 263*, 1425-1429.
7. Frauendorf, C., and Jaschke, A. (2001) Detection of small organic analytes by fluorescing molecular switches, *Bioorganic & medicinal chemistry 9*, 2521-2524.
8. Soukup, G. A., Emilsson, G. A., and Breaker, R. R. (2000) Altering molecular recognition of RNA aptamers by allosteric selection, *Journal of molecular biology 298*, 623-632.
9. Soukup, G. A., and Breaker, R. R. (1999) Design of allosteric hammerhead ribozymes activated by ligand-induced structure stabilization, *Structure 7*, 783-791.
10. Soukup, G. A., and Breaker, R. R. (1999) Engineering precision RNA molecular switches, *Proceedings of the National Academy of Sciences of the United States of America 96*, 3584-3589.
11. Tang, J., and Breaker, R. R. (1997) Rational design of allosteric ribozymes, *Chemistry & biology 4*, 453-459.
12. Soukup, G. A., and Breaker, R. R. (1999) Nucleic acid molecular switches, *Trends in biotechnology 17*, 469-476.
13. Vaish, N. K., Dong, F., Andrews, L., Schweppe, R. E., Ahn, N. G., Blatt, L., and Seiwert, S. D. (2002) Monitoring post-translational modification of proteins with allosteric ribozymes, *Nature biotechnology 20*, 810-815.
14. Srinivasan, J., Cload, S. T., Hamaguchi, N., Kurz, J., Keene, S., Kurz, M., Boomer, R. M., Blanchard, J., Epstein, D., Wilson, C., and Diener, J. L. (2004) ADP-specific sensors enable universal assay of protein kinase activity, *Chemistry & biology 11*, 499-508.
15. Seetharaman, S., Zivarts, M., Sudarsan, N., and Breaker, R. R. (2001) Immobilized RNA switches for the analysis of complex chemical and biological mixtures, *Nature biotechnology 19*, 336-341.
16. Yin, B. C., Ye, B. C., Tan, W., Wang, H., and Xie, C. C. (2009) An allosteric dual-DNAzyme unimolecular probe for colorimetric detection of copper(II), *Journal of the American Chemical Society 131*, 14624-14625.
17. Roth, A., and Breaker, R. R. (2009) The structural and functional diversity of metabolite-binding riboswitches, *Annual review of biochemistry 78*, 305-334.
18. Weinberg, Z., Nelson, J. W., Lunse, C. E., Sherlock, M. E., and Breaker, R. R. (2017) Bioinformatic analysis of riboswitch structures uncovers variant classes with altered ligand specificity, *Proceedings of the National Academy of Sciences of the United States of America 114*, E2077-E2085.
19. Mori, Y., Nagamine, K., Tomita, N., and Notomi, T. (2001) Detection of loop-mediated isothermal amplification reaction by turbidity derived from magnesium pyrophosphate formation, *Biochemical and biophysical research communications 289*, 150-154.

20. Nagamine, K., Hase, T., and Notomi, T. (2002) Accelerated reaction by loop-mediated isothermal amplification using loop primers, *Molecular and cellular probes 16*, 223-229.
21. Van Ness, J., Van Ness, L. K., and Galas, D. J. (2003) Isothermal reactions for the amplification of oligonucleotides, *Proceedings of the National Academy of Sciences of the United States of America 100*, 4504-4509.
22. Notomi, T., Okayama, H., Masubuchi, H., Yonekawa, T., Watanabe, K., Amino, N., and Hase, T. (2000) Loop-mediated isothermal amplification of DNA, *Nucleic acids research 28*, E63.
23. Gill, P., and Ghaemi, A. (2008) Nucleic acid isothermal amplification technologies: a review, *Nucleosides, nucleotides & nucleic acids 27*, 224-243.
24. Cheng, X., Liu, X., Bing, T., Cao, Z., and Shangguan, D. (2009) General peroxidase activity of G-quadruplex-hemin complexes and its application in ligand screening, *Biochemistry 48*, 7817-7823.
25. Ohnishi, A., Kato, M., Kojima, J., Ushiama, H., Yoneko, M., and Kawai, H. (2003) Differential pharmacokinetics of theophylline in elderly patients, *Drugs & aging 20*, 71-84.
26. Ferapontova, E. E., Olsen, E. M., and Gothelf, K. V. (2008) An RNA aptamer-based electrochemical biosensor for detection of theophylline in serum, *Journal of the American Chemical Society 130*, 4256-4258.
27. Nirogi, R. V., Kandikere, V. N., Shukla, M., Mudigonda, K., and Ajjala, D. R. (2007) A simple and rapid HPLC/UV method for the simultaneous quantification of theophylline and etofylline in human plasma, *Journal of chromatography. B, Analytical technologies in the biomedical and life sciences 848*, 271-276.
28. Kawai, M., and Kato, M. (2000) Theophylline for the treatment of bronchial asthma: present status, *Methods and findings in experimental and clinical pharmacology 22*, 309-320.
29. Darty, K., Denise, A., and Ponty, Y. (2009) VARNA: Interactive drawing and editing of the RNA secondary structure, *Bioinformatics 25*, 1974-1975.
30. Fedor, M. J., and Uhlenbeck, O. C. (1992) Kinetics of intermolecular cleavage by hammerhead ribozymes, *Biochemistry 31*, 12042-12054.
31. Ruffner, D. E., Stormo, G. D., and Uhlenbeck, O. C. (1990) Sequence requirements of the hammerhead RNA self-cleavage reaction, *Biochemistry 29*, 10695-10702.
32. Zhao, Y., Chen, F., Li, Q., Wang, L., and Fan, C. (2015) Isothermal Amplification of Nucleic Acids, *Chemical reviews 115*, 12491-12545.
33. Zhao, Y., Zhou, L., and Tang, Z. (2013) Cleavage-based signal amplification of RNA, *Nature communications 4*, 1493.
34. Nie, J., Zhang, D. W., Tie, C., Zhou, Y. L., and Zhang, X. X. (2014) G-quadruplex based two-stage isothermal exponential amplification reaction for label-free DNA colorimetric detection, *Biosensors & bioelectronics 56*, 237-242.
35. Tan, E., Erwin, B., Dames, S., Ferguson, T., Buechel, M., Irvine, B., Voelkerding, K., and Niemz, A. (2008) Specific versus nonspecific isothermal DNA amplification through thermophilic polymerase and nicking enzyme activities, *Biochemistry 47*, 9987-9999.
36. Khvorova, A., Lescoute, A., Westhof, E., and Jayasena, S. D. (2003) Sequence elements outside the hammerhead ribozyme catalytic core enable intracellular activity, *Nature structural biology 10*, 708-712.
37. Stoltenburg, R., Krafcikova, P., Viglasky, V., and Strehlitz, B. (2016) G-quadruplex aptamer targeting Protein A and its capability to detect Staphylococcus aureus demonstrated by ELONA, *Scientific reports 6*, 33812.
38. Liu, J., and Lu, Y. (2006) Preparation of aptamer-linked gold nanoparticle purple aggregates for colorimetric sensing of analytes, *Nature protocols 1*, 246-252.

39. Li, X., Cheng, R., Shi, H., Tang, B., Xiao, H., and Zhao, G. (2016) A simple highly sensitive and selective aptamer-based colorimetric sensor for environmental toxins microcystin-LR in water samples, *Journal of hazardous materials 304*, 474-480.
40. Chavez, J. L., Lyon, W., Kelley-Loughnane, N., and Stone, M. O. (2010) Theophylline detection using an aptamer and DNA-gold nanoparticle conjugates, *Biosensors & bioelectronics 26*, 23-28.
41. Li, W., Jiang, W., and Wang, L. (2016) Self-locked aptamer probe mediated cascade amplification strategy for highly sensitive and selective detection of protein and small molecule, *Analytica chimica acta 940*, 1-7.
42. Pene, F., Courtine, E., Cariou, A., and Mira, J. P. (2009) Toward theragnostics, *Critical care medicine 37*, S50-58.
43. Hopkins, M. E., and MacKenzie-Ross, R. V. (2016) Case Report: The risks associated with chronic theophylline therapy and measures designed to improve monitoring and management, *BMC pharmacology & toxicology 17*, 13.
44. Chen, A., and Yang, S. (2015) Replacing antibodies with aptamers in lateral flow immunoassay, *Biosensors & bioelectronics 71*, 230-242.
45. Yetisen, A. K., Akram, M. S., and Lowe, C. R. (2013) Paper-based microfluidic point-of-care diagnostic devices, *Lab on a chip 13*, 2210-2251.
46. Weigl, B., Domingo, G., Labarre, P., and Gerlach, J. (2008) Towards non- and minimally instrumented, microfluidics-based diagnostic devices, *Lab on a chip 8*, 1999-2014.
47. Chin, C. D., Linder, V., and Sia, S. K. (2012) Commercialization of microfluidic point-of-care diagnostic devices, *Lab on a chip 12*, 2118-2134.
48. Tsui, N. B., Ng, E. K., and Lo, Y. M. (2002) Stability of endogenous and added RNA in blood specimens, serum, and plasma, *Clinical chemistry 48*, 1647-1653.
49. Liu, X., Freeman, R., Golub, E., and Willner, I. (2011) Chemiluminescence and chemiluminescence resonance energy transfer (CRET) aptamer sensors using catalytic hemin/G-quadruplexes, *ACS nano 5*, 7648-7655.
50. Sachais, B. S., Litvinov, R. I., Yarovoi, S. V., Rauova, L., Hinds, J. L., Rux, A. H., Arepally, G. M., Poncz, M., Cuker, A., Weisel, J. W., and Cines, D. B. (2012) Dynamic antibody-binding properties in the pathogenesis of HIT, *Blood 120*, 1137-1142.
51. Faulkner, A. E., Skoff, T. H., Tondella, M. L., Cohn, A., Clark, T. A., and Martin, S. W. (2016) Trends in Pertussis Diagnostic Testing in the United States, 1990 to 2012, *The Pediatric infectious disease journal 35*, 39-44.
52. Li, W. J., Chen, X. M., Nie, X. Y., Lin, X. X., Cheng, Y. J., Hu, C. H., Du, Z. M., Dong, Y. G., Ma, H., and Wu, S. H. (2015) Early diagnostic and prognostic utility of high-sensitive troponin assays in acute myocardial infarction: a meta-analysis, *Internal medicine journal 45*, 748-756.
53. Larsen, S. A., Steiner, B. M., and Rudolph, A. H. (1995) Laboratory diagnosis and interpretation of tests for syphilis, *Clinical microbiology reviews 8*, 1-21.
54. Wang, G., Sun, Y., Zhang, K., Jia, T., Hao, M., Zhang, D., Chang, L., Zhang, L., Zhang, R., Lin, G., Peng, R., and Li, J. (2015) External Quality Assessment of Molecular Detection of Ebola Virus in China, *PloS one 10*, e0132659.
55. Cameron, D. J., Johnson, L. B., and Maloney, E. L. (2014) Evidence assessments and guideline recommendations in Lyme disease: the clinical management of known tick bites, erythema migrans rashes and persistent disease, *Expert review of anti-infective therapy 12*, 1103-1135.
56. Jaax, M. E., Krauel, K., Marschall, T., Brandt, S., Gansler, J., Furll, B., Appel, B., Fischer, S., Block, S., Helm, C. A., Muller, S., Preissner, K. T., and Greinacher, A. (2013) Complex formation with nucleic acids and aptamers alters the antigenic properties of platelet factor 4, *Blood 122*, 272-281.

57. Jo, H., Gu, H., Jeon, W., Youn, H., Her, J., Kim, S. K., Lee, J., Shin, J. H., and Ban, C. (2015) Electrochemical aptasensor of cardiac troponin I for the early diagnosis of acute myocardial infarction, *Analytical chemistry 87*, 9869-9875.
58. Liu, X., Wang, F., Aizen, R., Yehezkeli, O., and Willner, I. (2013) Graphene oxide/nucleic-acid-stabilized silver nanoclusters: functional hybrid materials for optical aptamer sensing and multiplexed analysis of pathogenic DNAs, *Journal of the American Chemical Society 135*, 11832-11839.
59. Binning, J. M., Wang, T., Luthra, P., Shabman, R. S., Borek, D. M., Liu, G., Xu, W., Leung, D. W., Basler, C. F., and Amarasinghe, G. K. (2013) Development of RNA aptamers targeting Ebola virus VP35, *Biochemistry 52*, 8406-8419.